

## ORIGINAL PAPER

# Ataluren improves myelopoiesis and neutrophil chemotaxis by restoring ribosome biogenesis and reducing p53 levels in Shwachman–Diamond syndrome cells

Marco Cipolli<sup>1</sup> | Christian Boni<sup>1</sup> | Marianna Penzo<sup>2</sup> | Isabella Villa<sup>3</sup> |  
 Simona Bolamperti<sup>3</sup> | Elena Baldisseri<sup>1</sup> | Annalisa Frattini<sup>4,5</sup> | Giovanni Porta<sup>5</sup> |  
 Martina Api<sup>6</sup> | Nora Selicato<sup>1</sup> | Pamela Rocca<sup>5</sup> | Daniela Pollutri<sup>2</sup> |  
 Elena Marinelli Busilacchi<sup>7</sup> | Antonella Poloni<sup>7</sup> | Nicole Caporelli<sup>6</sup> | Giovanna D'Amico<sup>8</sup> |  
 Anna Pegoraro<sup>1</sup> | Simone Cesaro<sup>9</sup> | Usua Oyarbide<sup>10</sup> |  
 Antonio Vella<sup>11</sup> | Giuseppe Lippi<sup>12</sup>  | Seth J. Corey<sup>10</sup> | Roberto Valli<sup>5</sup>  |  
 Alessandro Polini<sup>13</sup> | Valentino Bezzeri<sup>1,12</sup>  

<sup>1</sup>Cystic Fibrosis Center, Azienda Ospedaliera Universitaria Integrata, Verona, Italy

<sup>2</sup>Department of Medical and Surgical Sciences (DIMEC) and Center for Applied Biomedical Research (CRBA), Alma Mater Studiorum University of Bologna, Bologna, Italy

<sup>3</sup>Institute of Endocrine and Metabolic Sciences, Endocrine and Osteometabolic Lab, IRCCS San Raffaele Hospital, Milano, Italy

<sup>4</sup>Institute for Genetic and Biomedical Research (IRGB), UOS Milano CNR, Milano, Italy

<sup>5</sup>Department of Medicine and Surgery (DMC), Università degli Studi dell'Insubria, Varese, Italy

<sup>6</sup>Cystic Fibrosis Center, Azienda Ospedaliera Universitaria Ospedali Riuniti, Ancona, Italy

<sup>7</sup>Hematology Clinic, Università Politecnica delle Marche, AOU Ospedali Riuniti, Ancona, Italy

<sup>8</sup>Centro Tettamanti, Fondazione IRCCS San Gerardo dei Tintori, Monza, Italy

<sup>9</sup>Pediatric Hematology Oncology, Ospedale Donna Bambino, Azienda Ospedaliera Universitaria Integrata, Verona, Italy

<sup>10</sup>Departments of Cancer Biology and Pediatric Hematology/Oncology and Stem Cell Transplantation, Cleveland Clinic, Cleveland, Ohio, USA

<sup>11</sup>Unit of Immunology, Azienda Ospedaliera Universitaria Integrata, Verona, Italy

<sup>12</sup>Section of Clinical Biochemistry, Department of Engineering for Innovation Medicine, University of Verona, Verona, Italy

<sup>13</sup>Institute of Nanotechnology, National Research Council (CNR-NANOTEC), Lecce, Italy

## Correspondence

Valentino Bezzeri, Cystic Fibrosis Center,  
 Azienda Ospedaliera Universitaria Integrata,  
 P.le A. Stefani 1, Verona 37126, Italy.  
 Email: [valentino.bezzeri@univr.it](mailto:valentino.bezzeri@univr.it)

## Funding information

Associazione Italiana Sindrome di  
 Shwachman-Diamond; Ministero della Salute,  
 Grant/Award Number: GR-2016-02363570;  
 National Institutes of Health, Grant/Award  
 Number: R01 DK132812; VeloSano

## Summary

Shwachman–Diamond syndrome (SDS) is characterized by neutropenia, exocrine pancreatic insufficiency and skeletal abnormalities. SDS bone marrow haematopoietic progenitors show increased apoptosis and impairment in granulocytic differentiation. Loss of Shwachman–Bodian–Diamond syndrome (*SBDS*) expression results in reduced eukaryotic 80S ribosome maturation. Biallelic mutations in the *SBDS* gene are found in ~90% of SDS patients, ~55% of whom carry the c.183-184TA>CT nonsense mutation. Several translational readthrough-inducing drugs aimed at suppressing nonsense mutations have been developed. One of these, ataluren, has received approval in Europe for the treatment of Duchenne muscular dystrophy. We previously showed that ataluren can restore full-length *SBDS* protein synthesis in SDS-derived bone marrow cells. Here, we extend our preclinical study to assess the

Shwachman-Diamond Foundation US: <https://www.twitter.com/cureforafuture>; Telethon Italia Foundation: <https://www.twitter.com/TelethonItalia>; Cleveland Clinic: <https://www.twitter.com/ClevelandClinic>; Regione Veneto Government Institution: <https://www.twitter.com/RegioneVeneto>; COST action EuNet-INNOCHRON on chronic neutropenias: [https://www.twitter.com/eunet\\_innochron](https://www.twitter.com/eunet_innochron).

This is an open access article under the terms of the [Creative Commons Attribution-NonCommercial](https://creativecommons.org/licenses/by-nc/4.0/) License, which permits use, distribution and reproduction in any medium, provided the original work is properly cited and is not used for commercial purposes.

© 2023 The Authors. *British Journal of Haematology* published by British Society for Haematology and John Wiley & Sons Ltd.

functional restoration of SBDS capabilities in vitro and ex vivo. Ataluren improved 80S ribosome assembly and total protein synthesis in SDS-derived cells, restored myelopoiesis in myeloid progenitors, improved neutrophil chemotaxis in vitro and reduced neutrophil dysplastic markers ex vivo. Ataluren also restored full-length SBDS synthesis in primary osteoblasts, suggesting that its beneficial role may go beyond the myeloid compartment. Altogether, our results strengthened the rationale for a Phase I/II clinical trial of ataluren in SDS patients who harbour the nonsense mutation.

#### KEY WORDS

ataluren, inherited bone marrow failure syndromes, myelodysplastic syndromes, Shwachman–Diamond syndrome, translational readthrough-inducing drugs

## INTRODUCTION

Shwachman–Diamond syndrome (SDS) is an inherited bone marrow failure syndrome characterized by haematological disorders, exocrine pancreatic insufficiency and bone abnormalities.<sup>1</sup> In most cases, bone marrows of SDS patients are hypocellular with impaired myeloid maturation, resulting in neutropenia.<sup>2</sup> Anaemia and thrombocytopenia are less frequent.<sup>3</sup> Almost 15%–20% of patients develop myelodysplastic syndrome (MDS) and/or acute myeloid leukaemia (AML).<sup>4</sup> Increased cellular tumour antigen p53 levels have been reported in SDS-derived bone marrow haematopoietic progenitor cells<sup>5</sup> and osteoblasts (OBs).<sup>6</sup> Mutations in *TP53* may represent maladaptive stress and is associated with increased risk of leukaemic transformation. No pharmacological therapy aimed at improving haematopoiesis or reducing the MDS/AML risk in SDS patients has been developed so far, and haematopoietic stem cell (HSC) transplant remains the main option in these cases.

SDS is mostly caused by mutations in the Shwachman–Bodian–Diamond syndrome (*SBDS*) gene,<sup>7</sup> which encodes an assembly factor for the 80S eukaryotic ribosome.<sup>8,9</sup> Other causative genes have been reported with phenotypes at least partially overlapping SDS, also in combination with *SBDS* mutations in some cases.<sup>10</sup> More than half of SDS patients harbour the nonsense mutation c.183-184TA>CT (K62X) in one *SBDS* allele.<sup>7,11</sup>

A premature termination codon produces a truncated, loss-of-function protein. Alternatively, no hypomorphic protein is produced because the mRNA containing premature termination codons is generally removed by an endogenous mechanism known as nonsense mediated decay.<sup>12</sup>

Translational readthrough-inducing drugs (TRIDs) are arousing growing interest as promising approaches to suppress nonsense mutations in monogenic disorders.<sup>13</sup> Among TRIDs, ataluren (PTC124; PTC Therapeutics)<sup>14</sup> was recently approved for use in Duchenne muscular dystrophy (DMD) in Europe.<sup>15</sup> Of note, ataluren-mediated readthrough of a premature termination codon that produces neomorphic protein may be due to its inhibition of the release factor activity during translation. Ataluren can bind two different sites within the rRNA in the ribosome.<sup>16,17</sup>

In a pilot study, we found that ataluren can restore SBDS synthesis in bone marrow haematopoietic progenitor cells

and mesenchymal stromal cells isolated from 13 patients with SDS.<sup>18</sup> We provide here preclinical efficacy of ataluren in restoring functional SBDS protein levels in several primary cell models and cell lines obtained from an enlarged cohort of 29 patients carrying *SBDS* nonsense mutations. We assessed the effect of ataluren in restoring the correct eukaryotic ribosome 80S maturation in SDS cells, improving the myelopoiesis ex vivo in primary bone marrow mononuclear cells (BM-MNCs). Ataluren reduced dysplastic features of neutrophils and improved their chemotaxis. Since SDS is characterized also by extra-haematological disorders, such as skeletal abnormalities, we found that ataluren restored SBDS protein synthesis in primary OBs isolated from SDS patients.

## METHODS

### Patient recruitment

We recruited 30 SDS patients from the Azienda Ospedaliera Universitaria Integrata (AOUI), Verona (Italy) and the Azienda Ospedaliera Universitaria Ospedali Riuniti (AOUOR), Ancona (Italy). All recruited SDS patients have biallelic mutations in *SBDS* (Table 1).

### Human samples and cell cultures

Peripheral blood mononuclear cells (PBMCs) and BM-MNCs were isolated by Ficoll-Paque Plus gradient centrifugation (Sigma-Aldrich), following the manufacturer's protocol. Primary human OB cultures were established by means of a modified version of the Gehron Robey and Termine procedure<sup>19</sup> from bone remnants of BM biopsies obtained from SDS patients. Trabecular bone specimens of healthy donors were obtained from bone remnants of hip prosthetic surgery. After incubation at 37°C for 30 min with Joklik's modified MEM (Sigma-Aldrich) containing 0.5 mg/mL type IV collagenase (Sigma-Aldrich), bone pieces from each sample were cultured until confluence in complete Iscove's Modified Dulbecco Medium (IMDM; Sigma-Aldrich). Cells were used at the second passage to reduce genotype changes. Human lymphoblastoid cell

**TABLE 1** Genetics and clinical aspects of SDS patients enrolled in this study.

UPN	Sex	Age	Genotype	PMN (cell/mm <sup>3</sup> )	Phenotype	Cytogenetics
6	M	18	258+2T>C/101A>T	3110	PI, FTT, bone malformation, thrombocytopenia, cognitive impairment	46,XY del(20)q
15	F	29	258+2T>C/183-184TA>CT	1107	PI, recurrent infections, bone malformation	46,XX,i(7)(q10)
20	M	43	258+2T>C/183-184TA>CT	500	PI, FTT, bone malformation, thrombocytopenia, anaemia	46,XY del(20)q
24	F	29	258+2T>C/183-184TA>CT	500	PS, FTT, thrombocytopenia, anaemia	46,XX
26	M	19	258+2T>C/183-184TA>CT	490	PI, FTT, bone malformation, thrombocytopenia	46,XY
37	F	10	258+2T>C/183-184TA>CT	250	PI, FTT, recurrent infections	46,XX i(7)(q10)
38	M	11	258+2T>C/183-184TA>CT	1250	PI, FTT, HbF >2%, bone malformation	46,XY
39	M	43	258+2T>C/183-184TA>CT	1300	PI, FTT, recurrent infections, HbF >2%, bone malformation, thrombocytopenia, cognitive impairment	46,XY
40	F	17	258+2T>C/183-184TA>CT	1040	PI, FTT, recurrent infections, HbF >2%, bone malformation, thrombocytopenia, anaemia	46,XX i(7)(q10)
43	M	22	258+2T>C/258+533_459+403del	970	PI, FTT, bone malformation, thrombocytopenia, cognitive impairment	46,XY
45	M	16	258+2T>C/183-184TA>CT	1700	PI, FTT, recurrent infections, cognitive impairment	46,XY
47	M	14	258+2T>C/183-184TA>CT	520	PI, FTT, recurrent infections, bone malformation, thrombocytopenia	46,XY
51	F	9	258+2T>C/258+2T>C	4000	PI, FTT, bone malformation, cognitive impairment	46,XX
55	M	15*	258+2T>C/183-184TA>CT	200	PS, FTT, recurrent infections, HbF >2%, bone malformation, thrombocytopenia	46,XY
58	M	16	258+2T>C/183-184TA>CT	230	PI, FTT, HbF >2%, bone malformation, thrombocytopenia, anaemia	46,XY
67	M	11	258+2T>C/183-184TA>CT	500	PI, FTT, HbF >2%, bone malformation	46,XY
69	F	10	258+2T>C/183-184TA>CT	1170	PI, FTT, HbF >2%, anaemia, cognitive impairment	46,XX
72	M	30	258+2T>C/183-184TA>CT	430	PI, FTT, recurrent infections, bone malformation, thrombocytopenia, anaemia, cognitive impairment	46,XY
73	F	9	258+2T>C/183-184TA>CT	2160	PI, FTT, HbF >2%, thrombocytopenia	46,XX
74	M	11	258+2T>C/183-184TA>CT	1320	PI, FTT, HbF >2%, cognitive impairment	46,XY
75	F	10	258+2T>C/183-184TA>CT	2280	PI, FTT, HbF >2%, bone malformation, thrombocytopenia, cognitive impairment	46,XX
80	M	9	258+2T>C/183-184TA>CT	790	PI, FTT, recurrent infections, bone malformation, anaemia, cognitive impairment	46,XY
82	M	16	258+2T>C/183-184TA>CT	300	PI, FTT, recurrent infections, bone malformation, thrombocytopenia, anaemia, cognitive impairment	46,XY
85	M	27	258+2T>C/183-184TA>CT	2000	PS, HbF >2%, recurrent infections, bone malformation, thrombocytopenia, cognitive impairment	46,XY
87	M	18	258+2T>C/183-184TA>CT	1290	PI, FTT, recurrent infections, bone malformation, cognitive impairment	46,XY
90	F	10	258+2T>C/183-184TA>CT	250	PI, FTT, bone malformation, thrombocytopenia, anaemia, cognitive impairment	46,XX
99	M	40	258+2T>C/183-184TA>CT	390	PI, FTT, HbF >2%, recurrent infections, bone malformation, thrombocytopenia, anaemia, cognitive impairment	46,XY
106	M	39	258+2T>C/183-184TA>CT	1200	PI, FTT, bone malformation, anaemia	46,XY
108	M	19	258+2T>C/183-184TA>CT	1438	PS, FTT, bone malformation, anaemia	46,XY
147	F	5	258+2T>C/183-184TA>CT	250	PI, FTT, bone malformation	46,XX

Abbreviations: \*, deceased; FTT, failure to thrive; PMN, polymorphonuclear neutrophils; PI, pancreas insufficiency; PS, pancreas sufficiency; SDS, Shwachman–Diamond syndrome; UPN, unique patient number.

lines (LCLs) from both SDS patients and healthy donors (Table S1) were obtained as previously described<sup>20</sup> and cultured in complete RPMI-1640 (Sigma-Aldrich), whereas HEK293T were grown in complete eagle's minimum essential medium (Sigma-Aldrich).

## Western blot

Total protein extracts were loaded in 12% sodium dodecyl sulphate–polyacrylamide (SDS–PAGE) gel (Bio-Rad). Proteins were then transferred into nitrocellulose membranes (Bio-Rad) and incubated with the proper primary and secondary antibodies as previously reported<sup>18</sup> and extensively described in [Supplementary Methods](#).

## Plasmid engineering, transfections and immunofluorescence

Plasmid pcDNA3.1(+)-P2A-eGFP from GenScript Biotech Corporation has been engineered to include *SBDS* wild-type cDNA sequence followed by the self-cleavage P2A sequence and the *eGFP* gene as positive control of the transfections (Figure S1). The plasmid has then been mutagenized to introduce the c.183\_184TA>CT mutation in the *SBDS* cDNA sequence (see [Supplementary Methods](#)). HEK293T cells have been transfected with Polyplus jetOPTIMUS following the manufacturer's indications. Fluorescence microscopy was performed with an Olympus IX51 Inverted fluorescent microscope, equipped with U-RFL-T200 lamp and U-TV0.5XC-3 CCD Camera (Olympus). Image analysis was performed by analSYS^B 5.0 (Soft Imaging System).

## Protein synthesis assay (SUnSET)

For measuring protein synthesis, LCL (UPN58) was treated with DMSO (vehicle, 1:2000) or 2.5–5  $\mu$ M of ataluren for 24h. Subsequently, 1  $\mu$ M puromycin was added to the medium for 30 min. Cells were then lysed and western blot was performed as described above. Additional information about antibody dilution and data analysis is provided in the [Supplementary Methods](#).

## Colony assays

BM-MNCs were plated in duplicate at a density of  $1 \times 10^5$ /mL in 30-mm Petri dishes containing 1 mL of StemMACS HSC-CFU lite medium supplemented with 20 ng/mL granulocyte colony-stimulating factor (G-CSF; Filgrastim, Hospira). For treatment, DMSO (vehicle, 1:4000) or 2.5  $\mu$ M of ataluren were added to the medium. Granulocyte–macrophage colony-forming units (GM-CFU) and burst-forming unit-erythroid (BFU-E) were counted every 7 days using a SMZ1270 stereomicroscope (Nikon).

## Polysome profile analysis

Polysome profiles were analysed as previously described.<sup>21</sup> Briefly, cell lysates were loaded on a 15%–50% continuous sucrose gradient. Separation of cytoplasmic components was achieved by ultracentrifugation, and polysome profiles were monitored at 254 nm using an ISCO gradient fractionator system. Further details are provided in the [Supplementary Methods](#).

## Chemotaxis-on-chip

Flow-free microfluidic devices are described properly in [Supplementary Methods](#).<sup>22</sup> Briefly, freshly isolated BM-MNC were preincubated with DMSO (vehicle, 1:2000) or with 5  $\mu$ M of ataluren for 24h in complete IMDM (ThermoFisher Scientific) supplemented with 20 ng/mL of G-CSF. The chemotaxis-on-chip assay was performed injecting  $1.5 \times 10^4$  BM-MNC-derived neutrophils in the upper reservoir of the microfluidic device, meanwhile the chemotactic stimuli [100 ng/mL of interleukin-8 (IL-8) and 1  $\mu$ M of N-Formylmethionyl-leucyl-phenylalanine (fMLP); PeproTech] were injected in the lower reservoir (Figure 4A). Migration was recorded capturing images for 1h every minute using bright field time-lapse microscopy. Data were further analysed to quantitatively evaluate the movement of cells by the forward migration index (FMI) and centre of mass.

## Neutrophil dysplastic marker evaluation

Isolated neutrophils were supplemented with 20 ng/mL of G-CSF in the presence or absence of ataluren treatment, and after 24h, dysplastic markers were evaluated using a flow cytometer FACSCanto II (BD Biosciences). Further details are provided in the [Supplementary Methods](#).

## Statistical analysis

Normal distribution was evaluated by the Shapiro–Wilk test before performing parametric or non-parametric tests in each experiment. Independent group determination was analysed using two-tailed Student's *t*-test for paired or unpaired data. A  $p < 0.05$  was considered statistically significant. The statistical analysis was performed using Prism 7 (GraphPad).

## RESULTS

### Ataluren reduces p53 protein levels in SDS LCL

Ribosomal biogenesis is impaired in SDS-derived cells, as characterized by reduced 80S ribosome assembly.<sup>8,9</sup> Consequently, the overall protein synthesis capability has

been found severely reduced in SDS cells.<sup>23</sup> In SDS, the ribosome assembly defect is due to the loss of SBDS protein synthesis, impairing the molecular mechanism leading to the release of EIF6.<sup>24</sup> We incubated LCL obtained from SDS patients harbouring the nonsense mutation c.183-184TA>CT with ataluren to promote the expression of neomorphic SBDS protein. First, we verified the capability of ataluren to suppress the nonsense mutation in *SBDS* using two different techniques. Western blot analysis was performed in LCLs derived from six patients (UPN24, UPN26, UPN58, UPN75, UPN82 and UPN106) as previously reported,<sup>18</sup> whereas immunofluorescence was performed in HEK293T cells transfected with a plasmid encoding the human *SBDS* cDNA carrying the c.183-184TA>CT mutation with an eGFP sequence in frame (Figure S1). Our results confirmed that 2.5–5  $\mu$ M of ataluren can restore full-length SBDS protein synthesis in human cells by both immunofluorescence (Figure 1A; Figure S2A) and western blot (Figure 1B,C; Figure S2B). To exclude a potential out-of-target effect of ataluren on splicing mutations, we incubated LCL obtained from patient UPN51, homozygous for the c.258+2T>C *SBDS* variant, with 2.5–5 mM of ataluren for 24 h. As expected, ataluren cannot suppress splicing mutations (Figure S2C). In addition, ataluren did not increase SBDS protein levels in LCL obtained from healthy individuals (Figure S2D,E). Interestingly, it was recently reported that ataluren may promote nonsense-mutated *dystrophin* mRNA expression in skin fibroblasts from patients with DMD by partially restoring the nonsense mediated decay mechanism.<sup>25</sup> Considering these findings, we investigated the capability of ataluren to induce *SBDS* mRNA in SDS LCL. However, ataluren treatment showed no effect in restoring *SBDS* transcription (Figure S2F). As in other IBMFS,<sup>26</sup> SDS is characterized by elevated levels of p53 in haematopoietic and non-haematopoietic cells.<sup>5,6</sup> Here we show that p53 levels are elevated in LCL obtained from six SDS patients (UPN6, UPN26, UPN43, UPN58, UPN82 and UPN106) with different genotypes (Figure 1D,E; Figure S3A,B). Thus, we sought to evaluate whether ataluren could reduce the amount of p53 in LCL. Upon ataluren-dependent restoration of SBDS protein synthesis, we observed a statistically significant reduction (~50%) of p53 levels upon ataluren treatment for 24 h at both the concentrations tested (Figure 1F,G; Figure S3C).

### SDS LCL improves ribosome assembly and increases the total cellular protein synthesis after ataluren treatment

We next sought to evaluate the effect of ataluren on restoring ribosome biogenesis in SDS-derived LCL from UPN24 and UPN58. Ataluren (5  $\mu$ M) treatment significantly improved the eukaryotic 80S ribosome assembly (+49%) in SDS LCL without affecting healthy controls (Figure 2A–D). Performing SUNSET assays,<sup>27</sup> to evaluate the incorporation of puromycin in new synthesized polypeptide chains, we observed a reduction of the total protein synthesis in SDS

LCL compared with healthy controls (Figure S4A). Then, we sought to explore the effect of ataluren on the rescue of the total protein synthesis in SDS LCL obtained from UPN24 and UPN58. Ataluren (5 mM) significantly restored the total protein synthesis (+165%) in SDS LCL (Figure 2E–G). Ataluren did not improve the total protein synthesis in healthy donor-derived LCL (Figure S4B,C).

### Effect of ataluren on myeloid differentiation and neutrophil dysplasia in SDS BM-MNC

We analysed bone marrow aspirates obtained from 30 SDS patients and 16 healthy donors (Table S2). Based on results arisen from our pilot study,<sup>18</sup> we performed haematopoietic progenitor assays by incubating 2.5  $\mu$ M of ataluren in freshly isolated BM-MNCs ex vivo for 21 days. CFU-GM and erythroid colonies (BFU-E) were counted every 7 days. We observed that SDS haematopoietic progenitors produced 41% of myeloid and 20% of erythroid colonies compared to healthy donors (Figure 3A,B). Ataluren improved myeloid differentiation in SDS BM-MNCs, resulting in a significant 1.5-fold increase of CFU-GM after 14 days of incubation (Figure 3A). No effect of ataluren was observed on erythroid differentiation (Figure 3B). In addition, no significant effect of ataluren on SBDS synthesis was observed on healthy donor-derived BM-MNC at each time point. To verify that the improvement of myeloid colonies was associated with increased synthesis of SBDS, we checked SBDS protein levels on colonies isolated after 21 days of ataluren treatment. Ataluren showed no effect on SBDS synthesis in healthy donor-derived cells (Figure 3C), whereas it restored full-length neomorphic SBDS protein synthesis SDS cells (Figure 3D). Among all bone marrow aspirates tested, five (16%) did not respond to ataluren. We sought to investigate whether the increased myelopoiesis was also associated with reduced expression of dysplastic markers in neutrophils. We incubated SDS BM-MNC displaying higher levels of immature, dysplastic myelocytes in bone marrow with 20 ng/mL G-CSF in the presence of 5  $\mu$ M of ataluren for 24 h. Flow cytometry analysis was performed for granulocytic differentiation based on CD45, CD13, CD16 and CD11b, as previously described.<sup>28</sup> The analysis of the combination of CD16 expression with the granulocytic-monocytic lineage marker CD13 was used as a useful indicator of granulocytic differentiation<sup>29</sup> (Figure 3E). We analysed the expression of neutrophil dysplastic markers in BM-MNC obtained from nine SDS patients. A marked reversion of dysplastic condition (measured as CD11b-positive cells within the dysplastic myelocyte population) was observed in two cases (UPN37 and UPN80) out of three (Table 2) showing higher levels of dysplastic markers before treatment compared to healthy donors (Table S3). In the other six samples, which displayed lower levels of neutrophilic dysplastic markers, no significant effect of ataluren was observed (Table S4). In addition, in our experimental conditions (24 h), ataluren did not promote neutrophil differentiation in BM-MNC in vitro (Table 2; Table S4).

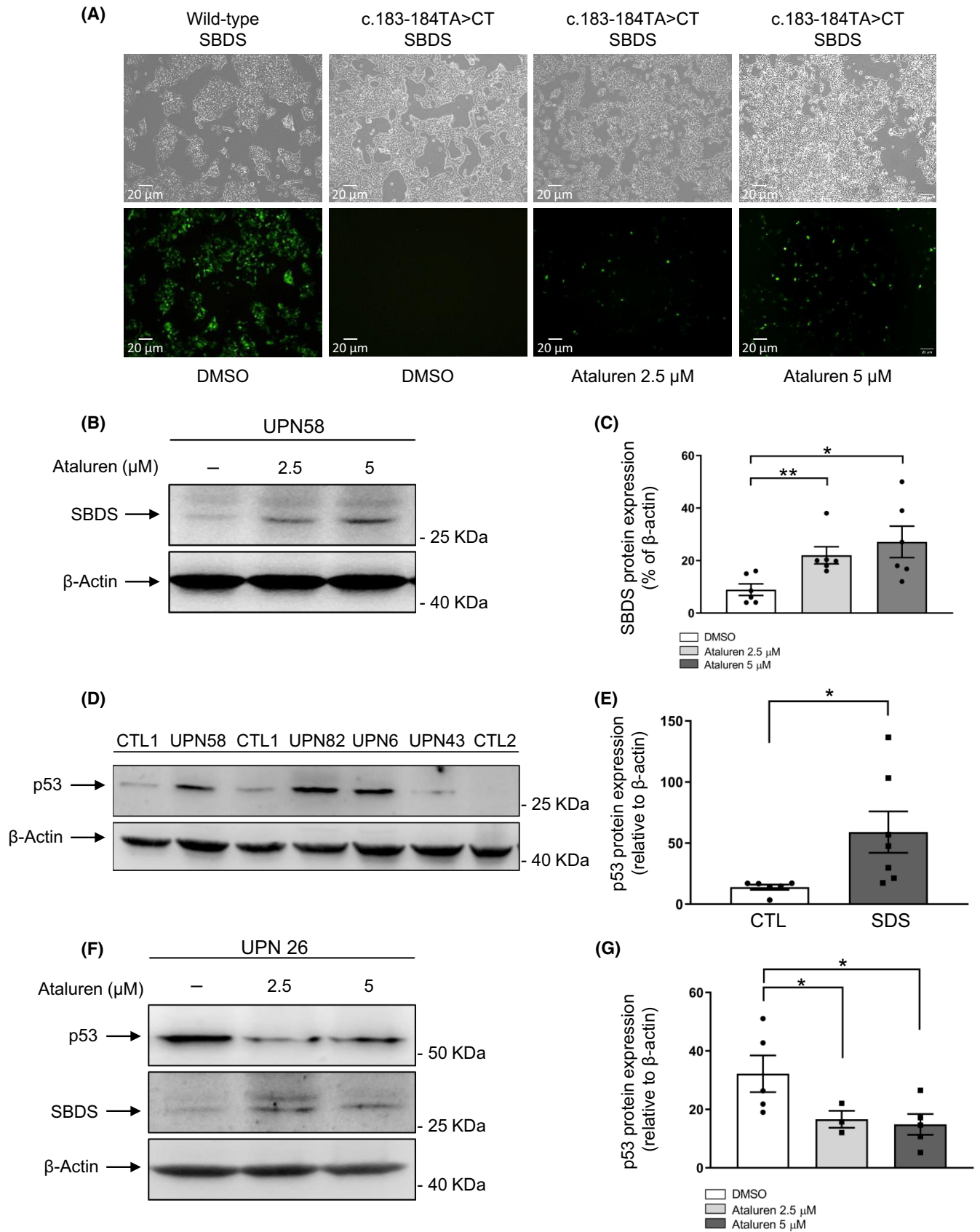


**FIGURE 1** Ataluren induces translational readthrough transfected HEK293T cells and in LCL carrying c.183-184TA>CT mutated *SBDS*, reducing p53 levels. (A) HEK293T cells transfected with the pcDNA3.1(+)-C-eGFP plasmid carrying the *SBDS* wild-type (wt) cDNA and *SBDS* carrying the c.183-184TA>CT stop mutation (magnification 10 $\times$ , images were acquired by Olympus IX51 Inverted fluorescent microscope equipped with Olympus U-TV0.5XC-3 CCD Camera). The wt *SBDS* plasmid has been used as positive control. The green signal appears after transcription of the chimeric wtSBDS-P2A-eGFP construct and the subsequent translation and cleavage of the two separated *SBDS* and eGFP proteins (Figure S1). The *SBDS* c.183-184TA>CT mutated plasmid produces the green signal only in case of readthrough of the PTC, induced by ataluren. (B) Representative experiment conducted on LCL generated from B cells of UPN58. Cells were incubated with ataluren 2.5–5  $\mu$ M or with DMSO (1:2000) as control, for 24 h. *SBDS* protein levels were detected by western blot analysis. (C) Scatter dot plots indicating the effect of ataluren on *SBDS* resynthesis in LCL obtained from UPN24, UPN26, UPN58, UPN75, UPN82 and UPN106 after 24 h of treatment. Data are the mean  $\pm$  SEM of six independent experiments. Normal distribution was tested by the Shapiro–Wilk test before running a two-tailed Student's *t*-test for paired data ( $*p < 0.05$ ;  $**p < 0.01$ ). (D) Representative experiment conducted on LCL from UPN6, UPN43, UPN58, UPN82 and healthy donors (CTL1 and CTL2). Cells were grown in RPMI 1640 medium supplemented with 10% FBS for 24 h. Then, p53 protein levels were detected by western blot analysis (D) and densitometry analysis was carried out (E). Scatter dot plots represent the mean  $\pm$  SEM of seven ( $n = 7$ ) experiments conducted on LCL derived from UPN6, UPN26, UPN43, UPN58, UPN82 and UPN106. (F) LCL obtained from UPN26 was treated with 2.5–5  $\mu$ M of ataluren for 24 h (representative experiment). Protein levels of p53 and *SBDS* were detected by western blot analysis, and densitometry analysis was performed (G). Scatter dot plots represent the mean  $\pm$  SEM of five independent experiments ( $n = 5$ ) conducted in LCL from UPN26, UPN58 and UPN82 as described in (F). During western blot analyses,  $\beta$ -actin was quantified as loading control. Normal distribution was tested by the Shapiro–Wilk test before running the two-tailed Student's *t*-test for paired data ( $*p < 0.05$ ). LCL, lymphoblastoid cell line; *SBDS*, Shwachman–Bodian–Diamond syndrome; UPN, unique patient number.

## Ataluren improves chemotaxis of neutrophils differentiated from SDS BM-MNC in vitro

While SDS neutrophils express normal levels of fMLP receptors throughout the plasma membrane, these cells are unable to orient in a spatial gradient of fMLP.<sup>30,31</sup> Random migration appears to be unaffected in SDS neutrophils, but the specific directionality through the chemotactic gradient due to fMLP is severely impaired.<sup>31</sup> To perform single-cell analysis of chemotaxis in SDS neutrophils, we developed a microfluidic device based on lab-on-chip technology<sup>32</sup> (Figure S5). FMI and centre of mass were then analysed. Chemotaxis-on-Chip assays confirmed that SDS neutrophils have a significantly impaired chemotaxis, both in terms of FMI and centre of mass, compared with healthy donor cells (Figure 4). We found that ataluren can enhance the fMLP/IL-8-dependent chemotaxis in SDS BM-MNC-derived neutrophils in vitro, restoring the correct directionality towards the chemotactic gradient without affecting chemotaxis in healthy donor-derived cells (Figure 4A–D; Videos S1–S9). In particular, in the presence of fMLP and IL-8, ataluren (5  $\mu$ M) improved both the FMI (5.6-fold increase, Figure 4B,C) and centre of mass (2.1-fold increase, Figure 4D) in SDS BM-MNC-derived neutrophils obtained from UPN26, UPN75, UPN80 and UPN147, compared with DMSO-treated controls.

## Ataluren restores *SBDS* protein expression in primary OB

To evaluate the efficacy of ataluren in restoring *SBDS* protein synthesis in non-haematopoietic tissues, we treated primary OBs obtained from four SDS patients (UPN24, UPN26, UPN72 and UPN106) with increasing doses of ataluren for a period from 24 to 96 h (Figure 5A,B; Figure S6). Ataluren efficacy varied among different primary OB cultures, showing restoration of synthesis of neomorphic *SBDS* in most samples tested. We observed that 10  $\mu$ M was the most effective concentration of ataluren in OBs within the 96 h, resulting

in a twofold increase of *SBDS* synthesis, whereas 5  $\mu$ M resulted in a slightly increased (+32%) resynthesis of *SBDS* (Figure 5C).

## DISCUSSION

SDS is a ribosomopathy caused by the loss of synthesis of a functional *SBDS* protein, which physically interacts with EFL1 to release EIF6 and facilitates 80S ribosome assembly.<sup>8,9</sup> The lack of expression of *SBDS* in SDS cells is mainly due to two peculiar mutations: the splicing variant c.258+2T>C in more than 90% of SDS patients, and the nonsense variant c.183-184TA>CT in ~55% of SDS patients.<sup>7,11</sup> Acting as a TRID, ataluren is approved in Europe for the treatment of DMD.<sup>15</sup> Here we report that ataluren restores full-length, neomorphic *SBDS* protein levels in haematopoietic-derived cells (LCL) and non-haematopoietic (OB) tissues. Ataluren-dependent synthesis of the neomorphic *SBDS* protein rescued myeloid differentiation, corrected granulocytic dysplasia and neutrophil chemotaxis, and reduced the exaggerated p53 levels.

Ataluren in vitro efficacy may vary depending on the type of tissue tested<sup>33</sup> and on the specific PTC sequence (UGA>UAG>UAA).<sup>14</sup> We have previously hypothesized that proliferating tissues, or metabolic active cells, may be easily targeted by ataluren, since we observed that ataluren-induced readthrough cannot be observed in primary PBMCs unless they are preincubated with phytohaemagglutinin in order to induce lymphocyte proliferation.<sup>18</sup> The presence of a unique PTC sequence (UGA) and the target tissue (proliferating haematopoietic progenitor/precursor cells) in SDS patients might constitute major strengths for the clinical use of ataluren in SDS. Ataluren can induce near-cognate insertion at the PTC, favouring a subset of tRNAs which lead to the incorporation of specific amino acids. In particular, Gln, Lys and Tyr are inserted at UAA stop codon, whereas Trp, Arg and Cys are inserted at UGA stop codon.<sup>34,35</sup> Thus, in SDS, we would predict the insertion of Trp, Arg and Cys in place of Lys at position 62 of the

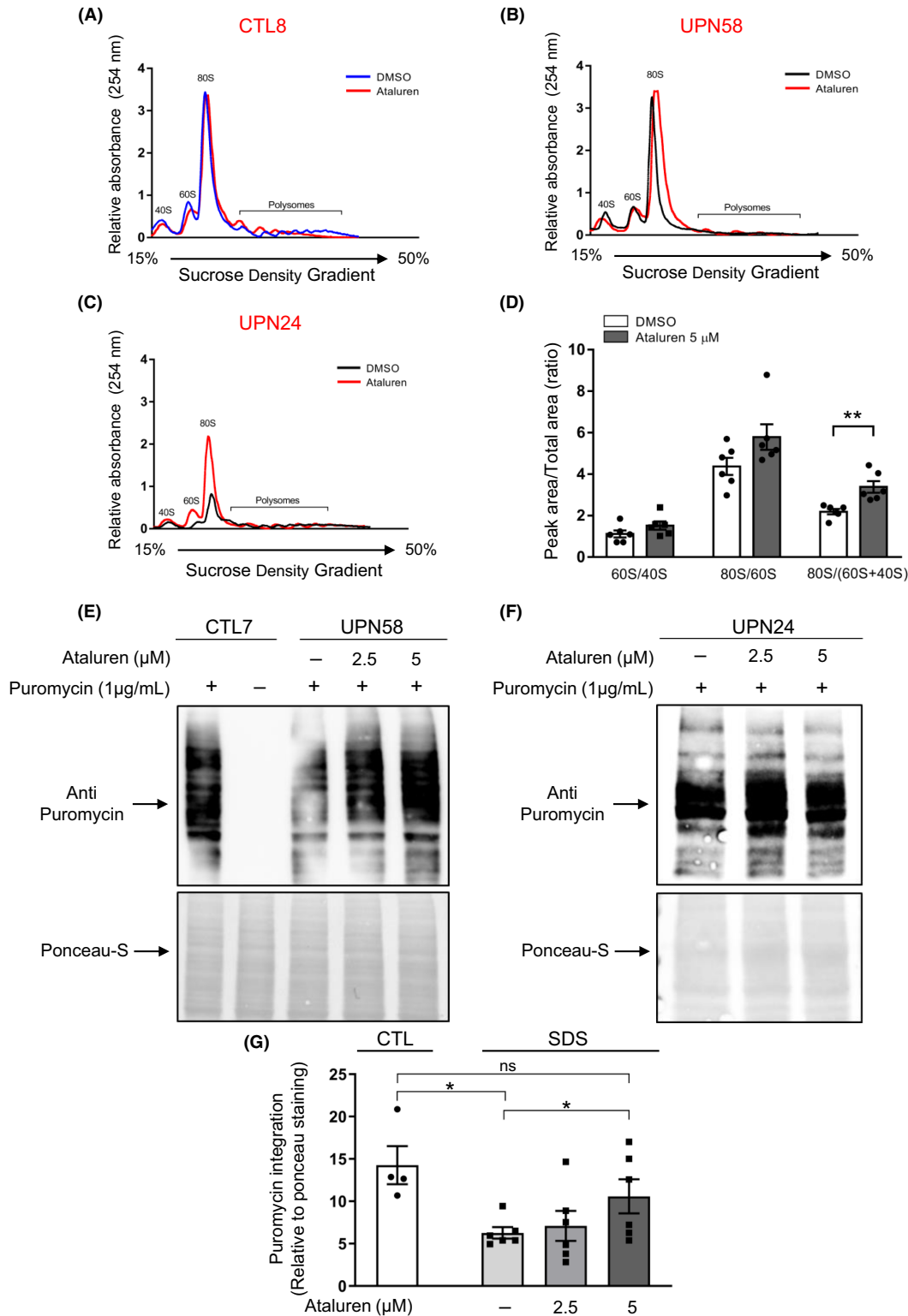


**FIGURE 2** Ataluren improves 80S ribosome assembly and whole protein synthesis in SDS LCL. (A–C) Representative polysome profiles of LCL obtained from healthy donor [CTL8 (A)], UPN58 (B) and UPN24 (C) were evaluated in the absence (DMSO, 1:2000) or presence of 5  $\mu$ M of ataluren for 24 h, by sucrose density gradient separation. (D) The ratio of peak areas:total areas of fractions 40S, 60S and 80S was calculated in six independent experiments (UPN58  $n=2$ , UPN24  $n=4$ ) as performed in (B, C). (E, F) Puromycin incorporation during protein synthesis was evaluated by SUNSET assay in LCL from UPN58 and UPN24 (representative experiments). (G) Scatter dot plots represent the mean  $\pm$  SEM of six independent experiments conducted in LCL from UPN58 ( $n=4$ ) and UPN24 ( $n=2$ ). Ponceau staining was used to evaluate the loading control. Normal distribution was tested by the Shapiro–Wilk test before running the two-tailed Student’s  $t$ -test for paired data ( $*p < 0.05$ ;  $**p < 0.01$ , ns = non-significant). LCL, lymphoblastoid cell line; SBDS, Shwachman–Bodian–Diamond syndrome; SDS, Shwachman–Diamond syndrome; UPN, unique patient number.



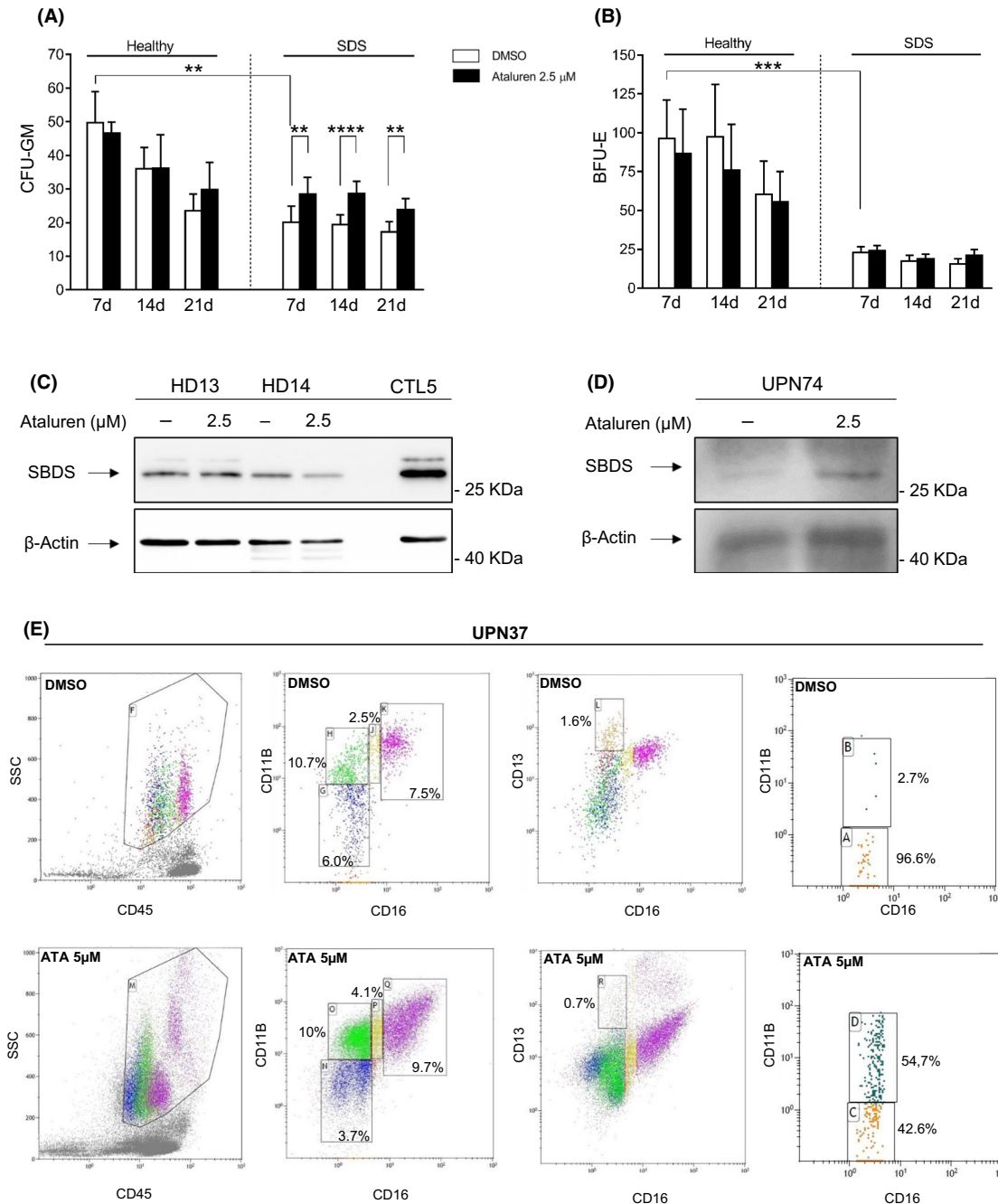


**FIGURE 3** Ataluren improves myelopoiesis ex vivo in BM-MNC isolated from SDS patients. (A, B) BM-MNCs isolated from bone marrow aspirates of SDS patients and healthy controls (as specified in Table S2) were seeded at a density of  $1 \times 10^5$  cells/mL in 3-cm Petri dishes containing StemMACS Lite medium supplemented with 20 ng/mL of G-CSF and incubated in the absence (DMSO, 1:4000) or in the presence of 2.5 μM of ataluren for 21 days at 37°C. CFU-GM (A) and BFU-E (B) were counted every 7 days. Histograms represent the mean  $\pm$  SEM of 32 bone marrow biopsies ( $n = 32$ ) isolated from 21 SDS patients. Normal distribution was tested by the Shapiro–Wilk test before running the two-tailed Student's *t*-test for paired data (\*\* $p < 0.01$ ; \*\*\* $p < 0.001$ ; \*\*\*\* $p < 0.0001$ ). (C) Representative western blot analysis of SBDS carried out in myeloid colonies obtained from HD13 and HD14 after 21 days of incubation in the absence (DMSO, 1:4000) or in the presence of 2.5 μM of ataluren as indicated in (A, B). Protein extracts obtained from CTL5 LCL were used as internal control of SBDS protein levels. (D) Representative western blot analysis of SBDS carried out in myeloid colonies obtained from UPN74 after 21 days of incubation in the absence (DMSO, 1:4000) or in the presence of 2.5 μM of ataluren as indicated in (A, B). (E) Freshly isolated bone marrow sample from UPN37 was depleted by red blood cells using osmotic lysis, and then incubated with or without (DMSO, 1:2000) 5 μM of ataluren for 24 h in IMDM supplemented with 10% FBS and 20 ng/mL G-CSF. Levels of CD11b, CD16, CD13 and CD45 were evaluated by flow cytometry (representative experiment). Flow cytometry analysis using the quadruple immunostaining for the granulocytic differentiation based on CD45, CD13, CD16 and CD11b was then performed. The analysis of the combination of CD16 expression with the granulocytic-monocytic lineage marker CD13 was used as a useful indicator of granulocytic differentiation. The percentage of each gated population is indicated within the plots. BFU-E, burst forming unit-erythroid; BM-MNC, bone marrow mononuclear cell; GM-CFU, granulocyte–macrophage colony-forming units; G-CSF, granulocyte colony-stimulating factor; IMDM, Iscove's Modified Dulbecco Medium; SDS, Shwachman–Diamond syndrome; SBDS, Shwachman–Bodian–Diamond syndrome; UPN, unique patient number.

**TABLE 2** Neutrophil dysplasia assessment before and after in vitro ataluren treatment.

UPN	Promyelo (%)		Myelo (%)		Metamyelo (%)		Granulo (%)		Dysplastic population CD13 <sup>+</sup> /CD16 <sup>-</sup> (%)			
									CD11b <sup>-</sup>		CD11b <sup>+</sup>	
37	6.0	3.7	<b>10.7</b>	<b>10.0</b>	2.5	4.1	7.5	9.7	<b>96.6</b>	<b>42.6</b>	<b>2.7</b>	<b>54.7</b>
58	0.62	0.8	8.54	10.02	1.24	1.09	19.65	19.78	83.74	84.31	11.50	10.79
80	2.43	1.67	22.86	21.2	3.6	3.17	15.24	13.84	<b>84.92</b>	<b>8.51</b>	<b>9.78</b>	<b>84.92</b>
Ataluren	-	+	-	+	-	+	-	+	-	+	-	+

Note: Neutrophil maturation stages were evaluated by flow cytometry analysis as already well established.<sup>28</sup> Gating strategy is depicted in Figure 3D. The analysis of the combination of CD16 expression with the granulocytic–monocytic lineage marker CD13 was employed as a useful indicator of granulocytic differentiation. Dysplastic condition was measured as CD11b-negative cells within the CD13<sup>+</sup> CD16<sup>-</sup> population. Patients showing neutrophil dysplastic features (UPN37, UPN58 and UPN80) before and after ataluren ex vivo treatment are reported. Values relative to healthy donors are showed in Table S3. Patients responding to ataluren treatment ex vivo are marked in bold.

Abbreviation: UPN, unique patient number.

nascent SBDS polypeptide chain. However, a limitation of this study is that a formal proof that a functional neomorphic SBDS protein is synthesized upon ataluren treatment has not been provided. Importantly, neomorphic proteins induced by ataluren treatment generally retain substantial function, regardless the different amino acids substitution.<sup>34</sup> Thus, the rescued expression of SBDS full-length protein, albeit neomorphic, should be followed by improved ribosome biogenesis and increased global protein synthesis capability. According to this assumption, ataluren-mediated rescue of SBDS synthesis led to a twofold increase in 80S mature ribosome amount in LCL obtained from SDS patients. This reflected a twofold increase in total protein synthesis capability, approximating normal levels.

Not all patients with SDS develop clinically important neutropenia or MDS/AML. A notable feature of both neutropenia and exocrine pancreatic insufficiency is their fluctuating severity. However, some do require G-CSF treatment (e.g. filgrastim). Here we analysed 30 bone marrow aspirates collected from a cohort of SDS patients carrying the c.183-184TA>CT nonsense mutation. Considering the rareness of SDS and the specific genotype selected for this study, this should be considered one of the most comprehensive studies on SDS human specimens conducted so far. CFU-GM were significantly improved in BM-MNCs upon treatment with ataluren for 7 (+53%), 14 (+88%) and 21 days (+73%). Although SDS patients carried the same nonsense mutation in *SBDS*, therefore harbouring the same stop codon sequence, we found five non-responding cases (16%). This was

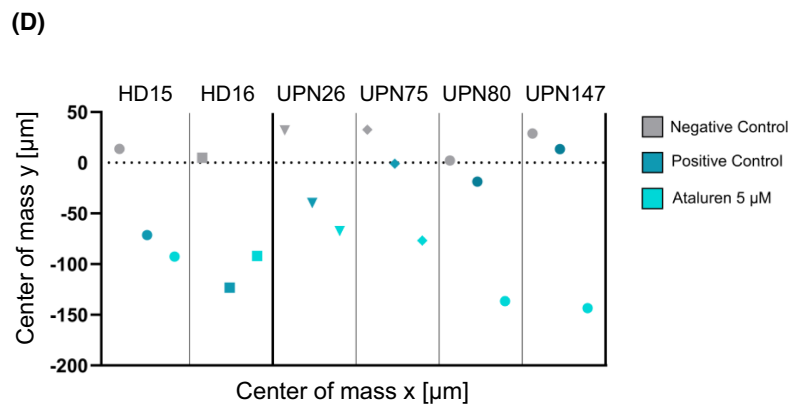
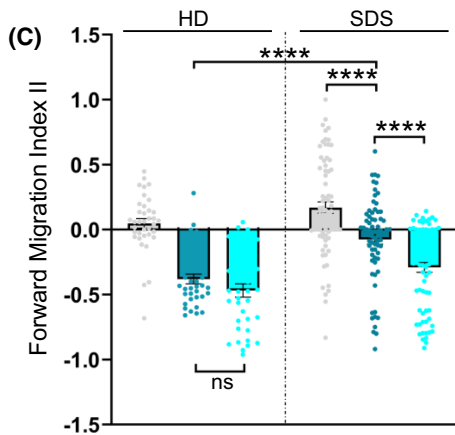
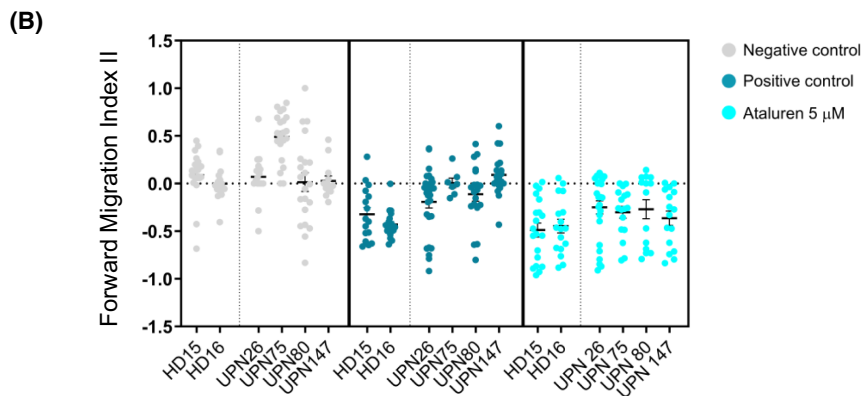
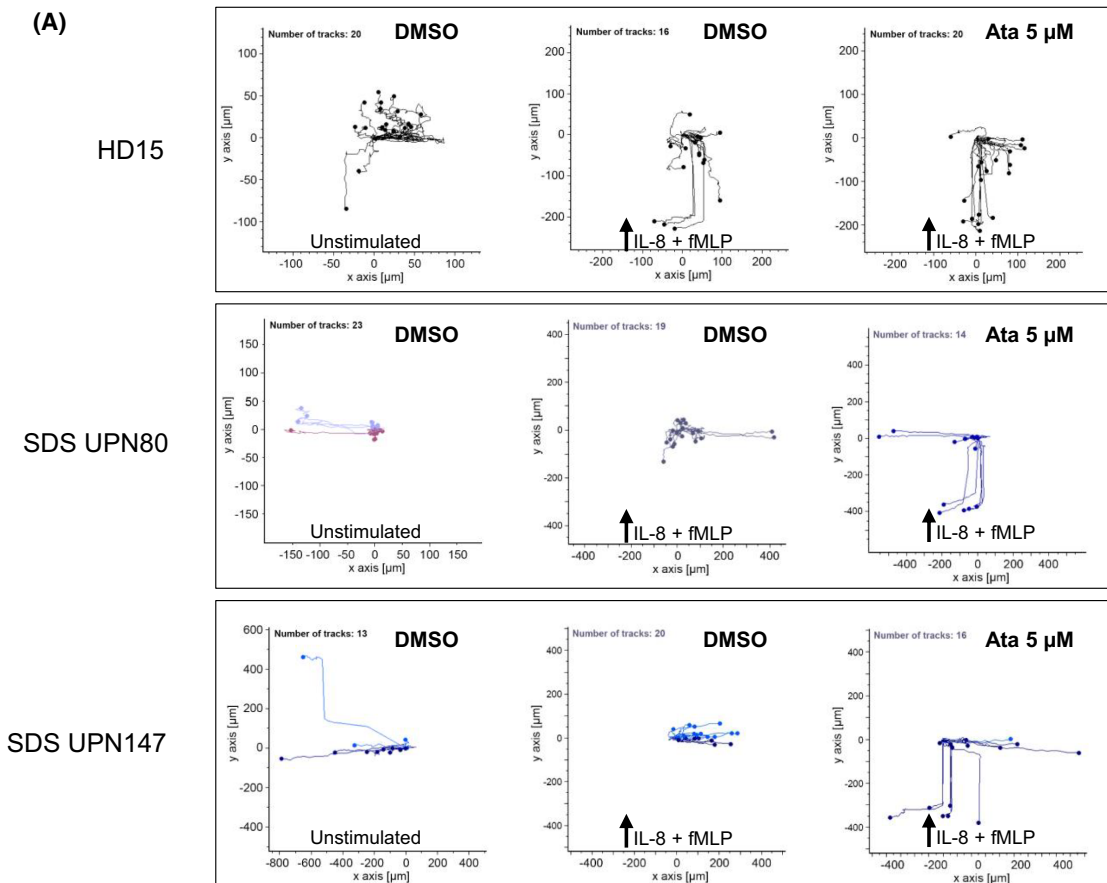
not surprising, because other investigations on DMD<sup>36</sup> and cystic fibrosis<sup>37</sup> had reported that ataluren's efficacy can vary even in patients carrying the same genotype. The mechanism underlying the lack of efficacy of ataluren in these cases remains unclear.<sup>33,34</sup>

No effect on erythropoiesis was observed upon ataluren treatment. Although *SBDS* expression is important for early erythroid differentiation,<sup>38</sup> both *SBDS* mRNA and protein levels rapidly decrease during erythroid maturation. After 5 days of in vitro differentiation, *SBDS* transcript was decreased by almost 80% in primary HSC CD133<sup>+</sup> cells. The same study showed that *SBDS* protein levels were almost undetectable after 4 days of in vitro differentiation in K562 cell line.<sup>38</sup> This suggests that in our experimental conditions (from 7 to 21 days of incubation), a clear effect on erythroid maturation may not be expected.

*SBDS* protein appears to be essential for the survival of granulocyte precursor cells in vitro.<sup>39</sup> We did not observe a significant increase in neutrophil maturation upon 24-h ataluren treatment, but we reported an almost complete reversion of dysplastic condition of SDS neutrophils in two out of three bone marrow aspirates which showed higher number of dysplastic neutrophils before treatment. Together with the reduced levels of p53 with ataluren treatment in vitro, these findings raise the issue of ataluren potential role in reducing the risk of leukaemic evolution. However, the small sample size decreases the power in this study.

SDS-derived neutrophils display a chemotaxis defect due to the altered F-actin polymerization.<sup>30</sup> Neutrophil

**FIGURE 4** Chemotaxis-on-Chip assay reveals that ataluren improves chemotaxis in SDS BM-MNC differentiated into neutrophils. BM-MNCs were isolated from bone marrow aspirates of four SDS patients (UPN26, UPN75, UPN80 and UPN147) and incubated in IMDM supplemented with 20 ng/mL G-CSF in the absence (DMSO, 1:2000) or in the presence of 5 μM of ataluren for 24 h to stimulate neutrophil differentiation. Neutrophil maturation marker CD66b was evaluated by flow cytometry before testing chemotaxis. Single-cell analysis of chemotaxis was performed on AVI video generated by capturing one image every minute for 60 min in time-lapse through a CCD camera connected to the microscope. Untreated BM-MNC-derived neutrophils were exposed to IL-8 and fMLP chemical gradient (positive control) or tested in the absence of chemotactic stimuli (negative control) to normalize random movements of the cells, regardless of chemotaxis. (A) Representative analysis of manual cell tracking conducted with ImageJ software in BM-MNC isolated from SDS patients (UPN80 and UPN147) and healthy donor HD15 and differentiated into neutrophils as described above, in the absence (DMSO, 1:2000) or in the presence of 5 μM of ataluren treatment. Each dot and line represent a single-cell analysis of cell movement under chemical gradient sustained by IL-8 and fMLP. (B) Forward migration index as calculated for each bone marrow sample tested. (C) Scatter dot plots are mean ± SEM independent experiments as depicted in (B). Normal distribution was tested by the Shapiro–Wilk test before running a two-tailed Student's *t*-test (\*\*\**p* < 0.0001). (D) The centre of mass has been calculated for each bone marrow sample tested under the same conditions indicated in (A). BM-MNC, bone marrow mononuclear cell; G-CSF, granulocyte colony-stimulating factor; IMDM, Iscove's Modified Dulbecco Medium; SDS, Shwachman–Diamond syndrome; UPN, unique patient number.



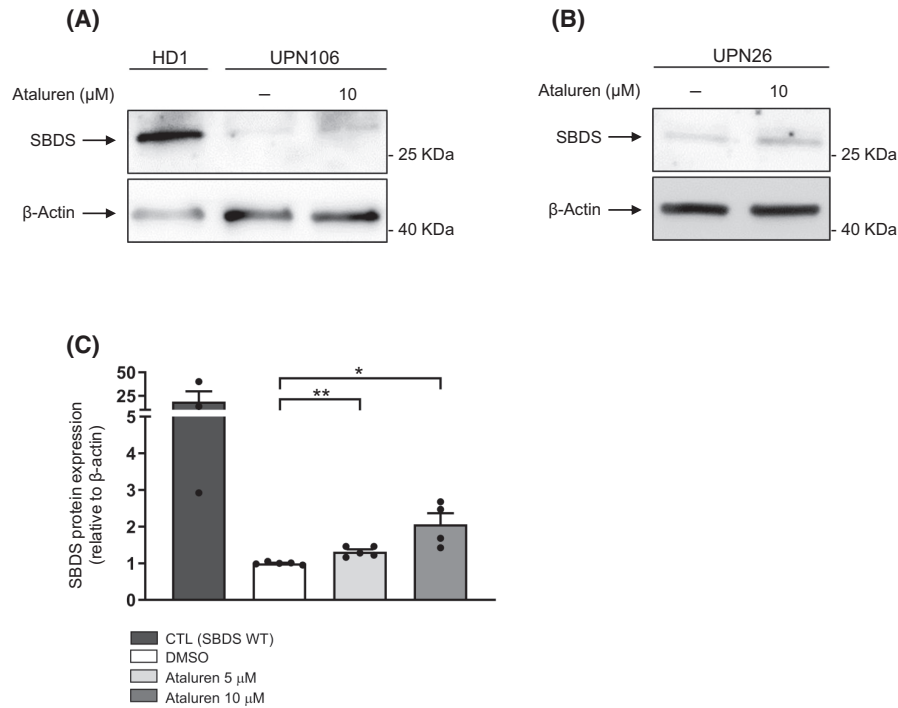


**FIGURE 5** Ataluren restores SBDS protein synthesis in primary osteoblasts isolated from SDS patients. Primary OBs were isolated from bone biopsies obtained from four SDS patients (UPN24, UPN26, UPN72 and UPN106) and healthy donors (HD1, HD2 and HD3). Cells (p1) were incubated in the absence (DMSO, 1:2000) or in the presence of 5–10 μM of ataluren for 24–96 h. Proteins were extracted in RIPA lysis buffer and western blot was performed to evaluate SBDS and β-actin levels. (A) Representative experiment conducted on OBs isolated from UPN106 at 24 h. (B) Representative experiment conducted on OBs isolated from UPN26 at 24 h. (C) Scatter dot plots indicating the maximal efficacy of ataluren treatment on SBDS resynthesis in OBs within the 96 h of treatment. Data are the mean ± SEM of 3–5 independent experiments. Normal distribution was tested by the Shapiro–Wilk test before running a two-tailed Student's *t*-test (\**p* < 0.05; \*\**p* < 0.01). OB, osteoblast; SBDS, Shwachman–Bodian–Diamond syndrome; SDS, Shwachman–Diamond syndrome; UPN, unique patient number.

chemotaxis impairment in SDS is not affected by the abnormal expression of chemokine receptors, nor by disruption of their signalling pathways, but mostly due to the inefficient orientation capability of neutrophil towards the chemotactic chemical gradient.<sup>31</sup> To properly evaluate neutrophil orientation capability under a chemotactic gradient, we sought to design a microfluidic device able to detect single-cell movement in real time due to chemotactic stimuli. Although other chemotaxis-on-chip assays based on mechanical flow are already commercially available, our device is optimized to work in flow-free conditions. Here we showed that ataluren treatment improved chemotaxis in BM-MNCs differentiated into neutrophils, increasing the FMI, which indicate the range of motion of cells towards the chemotactic chemical gradient, and the body mass centre, which measures the total movement of the cells in a two-dimensional environment. According to observations published by Stepanovic et al.,<sup>31</sup> our data confirm that untreated SDS neutrophils do not have impaired recognition of chemotactic factors, but they move randomly, independently from the chemoattractant chemical gradient. Interestingly, ataluren was able to improve the directionality of movement of SDS BM-MNC-derived neutrophils towards the chemotactic stimuli. Thus, ataluren may benefit those SDS patients with host defence deficiencies.<sup>3</sup>

Although OBs respond to higher doses of ataluren compared to haematopoietic cells, ataluren-dependent

improvement of SBDS levels in mesenchymal cells from bone matrix may further justify the clinical development of this drug. Since both dysregulation of *TP53* and stroma<sup>40,41</sup> may contribute to leukaemogenesis in SDS, ataluren might also reduce the risk of leukaemic progression in SDS patients. Overall, our study suggests that ataluren can be a promising personalized medicine approach for SDS patients carrying nonsense mutations. Preclinical results support a Phase I/II clinical trial of ataluren in SDS patients who harbour a nonsense mutation.

#### AUTHOR CONTRIBUTIONS

Marco Cipolli conceived the idea. Marco Cipolli and Valentino Bezzeri designed the research. Christian Boni, Marianna Penzo, Isabella Villa, Simona Bolamperti, Elena Baldisseri, Annalisa Frattini, Martina Api, Nora Selicato, Pamela Rocchia, Daniela Pollutri, Elena Marinelli Busilacchi, Antonella Poloni, Usua Oyarbide and Antonio Vella performed the research. Marco Cipolli, Nicole Caporelli, Alessandro Polini and Simone Cesaro recruited the patients. Alessandro Polini, Giovanna D'Amico and Antonio Vella carried out clinical immunology evaluation. Alessandro Polini designed and supervised chemotaxis-on-chip microfabrication. Roberto Valli, Antonella Poloni, Valentino Bezzeri and Giovanni Porta supervised the study. Valentino Bezzeri, Christian Boni, Marianna

Penzo, Antonella Poloni, Isabella Villa, Roberto Valli and Alessandro Polini analysed and interpreted data. Valentino Bezzeri and Seth J. Corey wrote the manuscript. Giuseppe Lippi internally revised the manuscript and contributed vital new reagents and analytical tools. All authors read and approved the manuscript.

### ACKNOWLEDGEMENTS

We are grateful to Benedetta Fabrizzi, Nadia Viola (AOUOR Ancona, Italy), Andrea Giustina (IRCCS San Raffaele, Milan) and Francesca Gervaso (CNR Nanotec, Lecce, Italy) for helpful discussions and facilitation of project management; to Gloria Tridello (AOUI Verona) for assisting in statistical analysis; to Cesare Danesino, Jacopo Morini (University of Pavia, Italy) and Claudio Sorio (University of Verona, Italy) for providing LCL; to Marisole Allegri (AOUOR Ancona, Italy) and Federica Quiri (AOUI Verona, Italy) for technical assistance.

### FUNDING INFORMATION

This work was partially supported by fellowships and grants from the Italian Ministry of Health, grant GR-2016-02363570 (V.B.), the Associazione Italiana Sindrome di Shwachman-Diamond (AISS to V.B., M.C. and R.V.), VeloSano (S.J.C. and U.O.) and NIH R01 DK132812 (S.J.C., U.O., M.C. and V.B.).

### CONFLICT OF INTEREST STATEMENT

V.B. and M.C. are co-inventors of the patent WO2018/050706 A1 Method of treatment of Shwachman–Diamond syndrome. The remaining authors declare no competing financial interests.

### DATA AVAILABILITY STATEMENT

All raw data have been included in supplementary information (Data S2). For original data, contact [valentino.bezzeri@univr.it](mailto:valentino.bezzeri@univr.it).

### ETHICS STATEMENT

This study was approved by the local Ethics Committees of the Azienda Ospedaliera Universitaria Integrata, Verona, Azienda Ospedaliera Universitaria Ospedali Riuniti, Ancona, and IRCCS San Raffaele Hospital, Milan (approval numbers 658CESC by AOUI-Verona, CERM 2018-82 by AOUIOR-Ancona, and BMU-Wnt, 15.07.2019 by IRCCS San Raffaele Hospital).

### PATIENT CONSENT STATEMENT

All recruited SDS patients were included only after the completion of informed consent documents as approved by the local Ethics Committees.

### ORCID

Giuseppe Lippi  <https://orcid.org/0000-0001-9523-9054>

Roberto Valli  <https://orcid.org/0000-0002-3209-8917>

Valentino Bezzeri  <https://orcid.org/0000-0002-6849-4487>

### TWITTER

Valentino Bezzeri  DrBezzeri

### REFERENCES

1. Myers KC, Furutani E, Weller E, Siegle B, Galvin A, Arsenault V, et al. Clinical features and outcomes of patients with Shwachman–Diamond syndrome and myelodysplastic syndrome or acute myeloid leukaemia: a multicentre, retrospective, cohort study. *Lancet Haematol.* 2020;7(3):e238–46.
2. Dror Y, Freedman MH. Shwachman–Diamond syndrome: an inherited preleukemic bone marrow failure disorder with aberrant hematopoietic progenitors and faulty marrow microenvironment. *Blood.* 1999;94(9):3048–54.
3. Bezzeri V, Vella A, Gennaro GD, Ortolani R, Nicolis E, Cesaro S, et al. Peripheral blood immunophenotyping in a large cohort of patients with Shwachman–Diamond syndrome. *Pediatr Blood Cancer.* 2019;66(5):e27597.
4. Donadieu J, Leblanc T, Bader Meunier B, Barkaoui M, Fenneteau O, Bertrand Y, et al. Analysis of risk factors for myelodysplasias, leukemias and death from infection among patients with congenital neutropenia. Experience of the French Severe Chronic Neutropenia Study Group. *Haematologica.* 2005;90(1):45–53.
5. Elghetany MT, Alter BP. p53 protein overexpression in bone marrow biopsies of patients with Shwachman–Diamond syndrome has a prevalence similar to that of patients with refractory anemia. *Arch Pathol Lab Med.* 2002;126(4):452–5.
6. Frattini A, Bolamperti S, Valli R, Cipolli M, Pinto RM, Bergami E, et al. Enhanced p53 levels are involved in the reduced mineralization capacity of osteoblasts derived from Shwachman–Diamond syndrome subjects. *Int J Mol Sci.* 2021;22(24):13331.
7. Boocock GR, Morrison JA, Popovic M, Richards N, Ellis L, Durie PR, et al. Mutations in SBDS are associated with Shwachman–Diamond syndrome. *Nat Genet.* 2003;33(1):97–101.
8. In K, Zaini MA, Müller C, Warren AJ, von Lindern M, Calkhoven CF. Shwachman–Bodian–Diamond syndrome (SBDS) protein deficiency impairs translation re-initiation from C/EBP $\alpha$  and C/EBP $\beta$  mRNAs. *Nucleic Acids Res.* 2016;44(9):4134–46.
9. Finch AJ, Hilcenko C, Basse N, Drynan LF, Goyenechea B, Menne TF, et al. Uncoupling of GTP hydrolysis from eIF6 release on the ribosome causes Shwachman–Diamond syndrome. *Genes Dev.* 2011;25(9):917–29.
10. Morini J, Nacci L, Babini G, Cesaro S, Valli R, Ottolenghi A, et al. Whole exome sequencing discloses heterozygous variants in the DNAJC21 and EFL1 genes but not in SRP54 in 6 out of 16 patients with Shwachman–Diamond syndrome carrying biallelic SBDS mutations. *Br J Haematol.* 2018;185:627–30.
11. Bezzeri V, Cipolli M. Shwachman–Diamond syndrome: molecular mechanisms and current perspectives. *Mol Diagn Ther.* 2018;23:281–90.
12. Kurosaki T, Popp MW, Maquat LE. Quality and quantity control of gene expression by nonsense-mediated mRNA decay. *Nat Rev Mol Cell Biol.* 2019;20(7):406–20.
13. Goldmann T, Overlack N, Möller F, Belakhov V, van Wyk M, Baasov T, et al. A comparative evaluation of NB30, NB54 and PTC124 in translational read-through efficacy for treatment of an USH1C nonsense mutation. *EMBO Mol Med.* 2012;4(11):1186–99.
14. Welch EM, Barton ER, Zhuo J, Tomizawa Y, Friesen WJ, Trifillis P, et al. PTC124 targets genetic disorders caused by nonsense mutations. *Nature.* 2007;447(7140):87–91.
15. Ryan NJ. Ataluren: first global approval. *Drugs.* 2014;74(14):1709–14.
16. Huang S, Bhattacharya A, Ghelfi MD, Li H, Fritsch C, Chenoweth DM, et al. Ataluren binds to multiple protein synthesis apparatus sites and competitively inhibits release factor-dependent termination. *Nat Commun.* 2022;13(1):2413.
17. Ng MY, Li H, Ghelfi MD, Goldman YE, Cooperman BS. Ataluren and aminoglycosides stimulate read-through of nonsense

- codons by orthogonal mechanisms. *Proc Natl Acad Sci U S A*. 2021;118(2):e2020599118.
18. Bezzeri V, Bardelli D, Morini J, Vella A, Cesaro S, Sorio C, et al. Ataluren-driven restoration of Shwachman–Bodian–Diamond syndrome protein function in Shwachman–diamond syndrome bone marrow cells. *Am J Hematol*. 2018;93(4):527–36.
  19. Robey PG, Termine JD. Human bone cells in vitro. *Calcif Tissue Int*. 1985;37(5):453–60.
  20. Bezzeri V, Vella A, Calcaterra E, Finotti A, Gasparello J, Gambari R, et al. New insights into the Shwachman–Diamond Syndrome-related haematological disorder: hyper-activation of mTOR and STAT3 in leukocytes. *Sci Rep*. 2016;6:33165.
  21. Galbiati A, Penzo M, Bacalini MG, Onofrillo C, Guerrieri AN, Garagnani P, et al. Epigenetic up-regulation of ribosome biogenesis and more aggressive phenotype triggered by the lack of the histone demethylase JHDM1B in mammary epithelial cells. *Oncotarget*. 2017;8(23):37091–103.
  22. De Vitis E, La Pesa V, Gervaso F, Romano A, Quattrini A, Gigli G, et al. A microfabricated multi-compartment device for neuron and Schwann cell differentiation. *Sci Rep*. 2021;11(1):7019.
  23. Calamita P, Miluzio A, Russo A, Pesce E, Ricciardi S, Khanim F, et al. SBDS-deficient cells have an altered homeostatic equilibrium due to translational inefficiency which explains their reduced fitness and provides a logical framework for intervention. *PLoS Genet*. 2017;13(1):e1006552.
  24. Warren AJ. Molecular basis of the human ribosomopathy Shwachman–Diamond syndrome. *Adv Biol Regul*. 2018;67:109–27.
  25. Amar-Schwartz A, Cohen Y, Elhaj A, Ben-Hur V, Siegfried Z, Karni R, et al. Inhibition of nonsense-mediated mRNA decay may improve stop codon read-through therapy for Duchenne muscular dystrophy. *Hum Mol Genet*. 2023;32(15):2455–63.
  26. Savage SA, Dufour C. Classical inherited bone marrow failure syndromes with high risk for myelodysplastic syndrome and acute myelogenous leukemia. *Semin Hematol*. 2017;54(2):105–14.
  27. Schmidt EK, Clavarino G, Ceppi M, Pierre P. SUNSET, a non-radioactive method to monitor protein synthesis. *Nat Methods*. 2009;6(4):275–7.
  28. Van Lochem EG, Van Der Velden VHJ, Wind HK, Te Marvelde JG, Westerdaal NAC, Van Dongen JJM. Immunophenotypic differentiation patterns of normal hematopoiesis in human bone marrow: reference patterns for age-related changes and disease-induced shifts. *Cytometry*. 2004;60B(1):1–13.
  29. Maynadié M, Picard F, Husson B, Chatelain B, Cornet Y, Le Roux G, et al. Immunophenotypic clustering of myelodysplastic syndromes. *Blood*. 2002;100(7):2349–56.
  30. Orelia C, Kuijpers TW. Shwachman–Diamond syndrome neutrophils have altered chemoattractant-induced F-Actin polymerization and polarization characteristics. *Haematologica*. 2009;94(3):409–13.
  31. Stepanovic V, Wessels D, Goldman FD, Geiger J, Soll DR. The chemotaxis defect of Shwachman–Diamond syndrome leukocytes. *Cell Motil Cytoskeleton*. 2004;57(3):158–74.
  32. Zhao W, Zhao H, Li M, Huang C. Microfluidic devices for neutrophil chemotaxis studies. *J Transl Med*. 2020;18(1):168.
  33. Thada V, Miller JN, Kovács AD, Pearce DA. Tissue-specific variation in nonsense mutant transcript level and drug-induced read-through efficiency in the Cln1(R151X) mouse model of INCL. *J Cell Mol Med*. 2016;20(2):381–5.
  34. Roy B, Friesen WJ, Tomizawa Y, Leszyk JD, Zhuo J, Johnson B, et al. Ataluren stimulates ribosomal selection of near-cognate tRNAs to promote nonsense suppression. *Proc Natl Acad Sci U S A*. 2016;113(44):12508–13.
  35. Chowdhury HM, Siddiqui MA, Kanneganti S, Sharmin N, Chowdhury MW, Nasim MT. Aminoglycoside-mediated promotion of translation readthrough occurs through a non-stochastic mechanism that competes with translation termination. *Hum Mol Genet*. 2018;27(2):373–84.
  36. Finkel RS, Flanigan KM, Wong B, Bönnemann C, Sampson J, Sweeney HL, et al. Phase 2a study of ataluren-mediated dystrophin production in patients with nonsense mutation Duchenne muscular dystrophy. *PLoS One*. 2013;8(12):e81302.
  37. Sermet-Gaudelus I, Boeck KD, Casimir GJ, Vermeulen F, Leal T, Mogenet A, et al. Ataluren (PTC124) induces cystic fibrosis transmembrane conductance regulator protein expression and activity in children with nonsense mutation cystic fibrosis. *Am J Respir Crit Care Med*. 2010;182(10):1262–72.
  38. Sen S, Wang H, Nghiem CL, Zhou K, Yau J, Taylor CS, et al. The ribosome-related protein, SBDS, is critical for normal erythropoiesis. *Blood*. 2011;118(24):6407–17.
  39. Yamaguchi M, Fujimura K, Toga H, Khwaja A, Okamura N, Chopra R. Shwachman–Diamond syndrome is not necessary for the terminal maturation of neutrophils but is important for maintaining viability of granulocyte precursors. *Exp Hematol*. 2007;35(4):579–86.
  40. Zambetti NA, Ping Z, Chen S, Kenswil KJG, Mylona MA, Sanders MA, et al. Mesenchymal inflammation drives genotoxic stress in hematopoietic stem cells and predicts disease evolution in human pre-leukemia. *Cell Stem Cell*. 2016;19(5):613–27.
  41. Zha J, Kunselman LK, Xie HM, Ennis B, Shah YB, Qin X, et al. Inducible Sbd deletion impairs bone marrow niche capacity to engraft donor bone marrow after transplantation. *Blood Adv*. 2022;6(1):108–20.

## SUPPORTING INFORMATION

Additional supporting information can be found online in the Supporting Information section at the end of this article.

**How to cite this article:** Cipolli M, Boni C, Penzo M, Villa I, Bolamperti S, Baldisseri E, et al. Ataluren improves myelopoiesis and neutrophil chemotaxis by restoring ribosome biogenesis and reducing p53 levels in Shwachman–Diamond syndrome cells. *Br J Haematol*. 2023;00:1–14. <https://doi.org/10.1111/bjh.19134>